Dislocation dynamics is chaotic

Deshpande, V.S.; Needleman, A.; van der Giessen, E.

Published in:
Scripta Materialia

DOI:
10.1016/S1359-6462(01)01135-6

Publication date:
2001

PERGAMON

Scripta Materialia 45 (2001) 1047–1053

www.elsevier.com/locate/scriptamat

Dislocation dynamics is chaotic

V.S. Deshpande[a], A. Needleman[a*], and E. Van der Giessen[b]

[a]*Division of Engineering, Brown University, Box D, Providence, RI 02912-9104, USA*

[b]*Department of Applied Physics, University of Groningen, Nyenborgh 4, 9747 AG Groningen, The Netherlands*

Received 8 June 2001; received in revised form 18 July 2001

Abstract

Numerical simulations of the dynamics of discrete dislocations exhibit chaotic behavior. The effect of chaos on the computed overall tensile stress–strain response is small, but the effect on the crack growth resistance is significant. © 2001 Acta Materialia Inc. Published by Elsevier Science Ltd. All rights reserved.

Keywords: Chaos; Dislocations, theory; Mechanical properties, plastic, fracture

Introduction

Plastic deformation in crystalline metals is often a consequence of the collective motion of large numbers of dislocations. In discrete dislocation models for plasticity, the dislocations are represented as line singularities in an elastic solid and the evolution of the dislocation structure is determined from their elastic interactions supplemented by a set of constitutive rules for short range interactions such as nucleation and annihilation [1–4]. Hamiltonian systems involving nonlinear many-body interactions are known to exhibit chaotic behavior: for example, gravitationally interacting point masses [5], molecular dynamics [6] and vortex dynamics [7]. Dissipative systems such as those characterized by the Lorenz equations [8] can also exhibit chaotic behavior. A signature of chaotic systems is that two almost identical starting configurations evolve very differently with time.

Experimental evidence for the existence of chaos in the plastic flow of crystalline metals has been reported in connection with the Portevin–Le Châtelier instability [9] and bursts of dislocation activity at the initiation of plasticity [10]. Here we present numerical simulations of the dynamics of discrete dislocations and demonstrate that dislocation dynamics itself can exhibit chaotic behavior (in previous work, phenomenological reaction–diffusion equations have been postulated to represent presumed

* Corresponding author. Tel.: +1-401-863-2863; fax: +1-401-863-1157.
E-mail address: needle@engin.brown.edu (A. Needleman).

PII: S1359-6462(01)01135-6

chaotic plastic flow, e.g. Refs. [11,12]). The chaos that emerges in some, but not all, of our calculations is a consequence of dislocation interactions and is thus a direct outcome of the physical mechanism of plastic flow. Furthermore, this chaos is not associated with a macroscopic instability.

Discrete dislocation formulation

The boundary value problem addressed first is sketched in Fig. 1. A plane strain strip of dimension $L = 16$ μm and $h = 4$ μm subjected to a prescribed displacement is analyzed using the discrete dislocation formulation in Refs. [2,4]. The crystal has isotropic elastic properties specified by the shear modulus $\mu = 26.3$ GPa and Poisson's ratio $\nu = 0.33$. Plastic deformation is assumed to occur by the motion of edge dislocations only, with Burgers vector magnitude $b = 0.25$ nm and there is no cross-slip so that dislocations remain on their slip planes. The magnitude of the glide velocity $v^{(I)}$ of dislocation I is prescribed to be linearly related to the Peach–Koehler force $f^{(I)}$ through the drag relation

$$v^{(I)} = \frac{1}{B} f^{(I)} \tag{1}$$

with $B = 10^{-4}$ Pa s and $f^{(I)}$ the glide component of the Peach–Koehler force,

$$f^{(I)} = b_i \left(\hat{\sigma}_{ij} + \sum_{J \neq I} \tilde{\sigma}_{ij}^{(J)} \right) m_j^{(I)}. \tag{2}$$

Here b_i is the Burgers vector, m_j^I is the slip plane normal, $\tilde{\sigma}_{ij}^{(J)}$ are the interaction stresses with the other dislocations and $\hat{\sigma}_{ij}$ are the image stresses that are due to the boundary conditions.

The crystal has a random distribution of dislocation sources and point obstacles. The sources mimic Frank–Read sources and generate a dislocation dipole when the magnitude of the Peach–Koehler force exceeds a critical value of $b\tau_{\text{nuc}}$ during a period of time t_{nuc}, with $\tau_{\text{nuc}} = 50$ MPa and $t_{\text{nuc}} = 10$ ns. The obstacles pin dislocations and release them once the Peach–Koehler force attains the obstacle strength $b\tau_{\text{obs}}$, where $\tau_{\text{obs}} = 150$ MPa. Annihilation of two dislocations with opposite Burgers vectors occurs when they approach each other within a critical annihilation distance $L_e = 6b$. Unless otherwise specified the calculations were carried out for a crystal with two slip systems

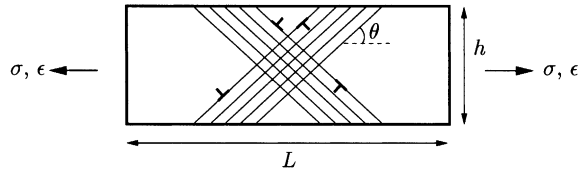

Fig. 1. Sketch of the boundary value problem analyzed.

at $\theta = \pm 30°$ as shown in Fig 1. The slip plane spacing is 100 Burgers vectors with a total of 202 slip planes. Initially, the crystal is dislocation free with 404 dislocation sources and 404 obstacles. A loading rate of $\dot{\epsilon} = 10^3\ \mathrm{s}^{-1}$ was employed.

A system is defined as chaotic if small perturbations in the initial configuration are amplified exponentially with time [13]. In particular, for a chaotic one-dimensional discrete system (a system characterized by a single variable x) two trajectories that are at x_0 and $x_0 + \delta_0$ at t_0, where $\delta_0 \ll x_0$, grow apart exponentially with time as

$$\delta(t) \approx \delta_0 \mathrm{e}^{\lambda t}. \tag{3}$$

The coefficient λ is known as the Lyapunov exponent of the system. For a multidimensional system the exponential deviation is characterized by as many Lyapunov exponents as the number of degrees of freedom of the system. A system behaves chaotically if it has at least one positive global Lyapunov exponent [13].

To calculate the deviation of nearby trajectories in the discrete dislocation dynamic simulations, the positions of the nucleation sites are perturbed with respect to a reference calculation. The separation of these two initially nearby trajectories is then evaluated based on the positions of corresponding dislocations in the two simulations. Dislocations are numbered in order of their nucleation times (with the positive dislocation in the generated dipole taken to be nucleated "first") and the norm of the separation of the trajectories $\|\delta\|$ is defined as

$$\|\delta(t)\| = \frac{1}{N} \sum_{I=1}^{N} \sqrt{\left(x_{\mathrm{p}}^{(I)}(t) - x_{\mathrm{u}}^{(I)}(t)\right)^2 + \left(y_{\mathrm{p}}^{(I)}(t) - y_{\mathrm{u}}^{(I)}(t)\right)^2}. \tag{4}$$

Here N is the number of dislocations (if the number of dislocations in the two simulations differ, N is taken to be the number of dislocations in the simulation with fewer dislocations at the given time [1]), and $x^{(I)}$ and $y^{(I)}$ the Cartesian coordinates of the Ith dislocation. The subscripts p, u denote the perturbed and unperturbed simulations, respectively. Coordinates of the dislocations that annihilate and exit the sample are taken as those of their annihilation point and exit point, respectively.

The evolution of $\|\delta\|$ with time is shown in Fig. 2a for the case where the nucleation sites were randomly perturbed by a maximum of $10^{-3}b$. After an initial delay of ≈ 0.75 μs the deviation of the trajectories grows exponentially before leveling off: at 0.75 μs four dislocations are present in each of the initially dislocation-free specimens. The finite size of the sample enforces a maximum value of $\|\delta\|$ and thus $\|\delta\|$ levels off at $\approx 2 \times 10^4 b = 5$ μm which is of the order of the size of the region analyzed. Note that although $\|\delta\|/b$ is relatively constant in the latter stages of the calculations, the number of dislocations is increasing as seen subsequently in Fig. 4b.

Possible reasons for this chaotic behavior are (i) the numerical scheme with the discrete integration procedure used is unstable and (ii) the underlying equations governing the dislocation motions are themselves chaotic. To explore these possibilities,

[1] This is an appropriate measure when the difference in the number of dislocations between the two solutions is small; before the curves level off in Fig. 2a this difference is six or fewer out of a total of more than 100.

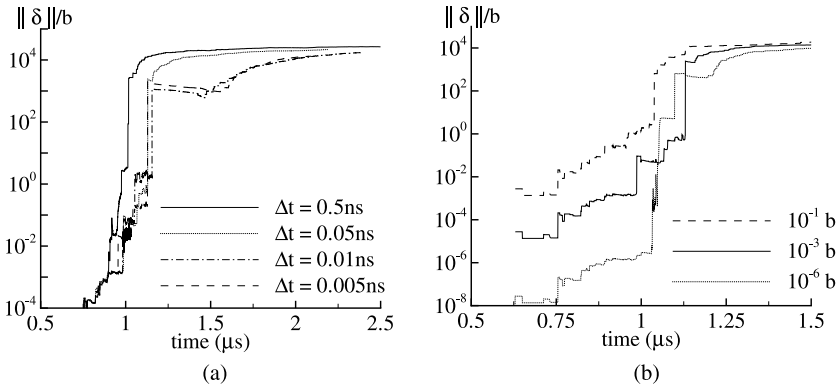

Fig. 2. (a) Time evolution of $\|\delta\|$ with nucleation sites perturbed by a maximum of $10^{-3}b$. Numerical results employing four time steps are shown. (b) Effect of the magnitude of the perturbations of the nucleation sites. The values in the legend denote the maximum levels of the random perturbations applied.

calculations were performed with time steps Δt ranging from 0.5 to 0.005 ns as shown in Fig. 2a. While the rate of divergence (i.e. the Lyapunov exponent) decreases as Δt is reduced from 0.5 to 0.01 ns, the difference for $\Delta t = 0.01$ and 0.005 ns is negligible. This suggests that the system has a positive Lyapunov exponent as $\Delta t \to 0$, indicating that the underlying equations governing the collective motion of dislocations are chaotic. In Fig. 2a the time step $\Delta t = 0.05$ ns captures the essential features of the behavior of the system. Thus, unless stated otherwise, results presented below were computed using $\Delta t = 0.05$ ns. Fig. 2b shows the effect of changing the magnitude of the maximum perturbation from $10^{-6}b$ to $10^{-1}b$. Again we see exponential growth of $\|\delta\|$ demonstrating the sensitive dependence on initial conditions.

We now show that chaos occurs even when dislocation nucleation is suppressed. In the simulations in Fig. 3 the specimen was strained until a prescribed number of dislocations were present in the sample. Two calculations were then carried out: (i) a reference calculation and (ii) a calculation with the initial positions of the dislocations perturbed by a maximum of $10^{-3}b$. Fig. 3 shows results for various values of the initial number of dislocations N. For $N = 264$ there is an initially high divergence rate followed by continuing divergence of the trajectories albeit at a lower rate. For $N = 86$ and 50 no divergence of the trajectories is seen, indicating that a minimum number of dislocations is required for chaotic behavior to set in when nucleation is suppressed. A calculation identical to the $N = 264$ case discussed above but with dislocation nucleation permitted is also shown in Fig. 3: a comparison between the two $N = 264$ cases reveals that the Lyapunov exponent is greatly enhanced when new dislocations nucleate. The Lyapunov exponent in the case of perturbed dislocations and with nucleation is approximately equal to that when the nucleation sites were perturbed (Fig. 2a), which indicates a negligible contribution to $\|\delta\|$ from any mismatch in the order of activation of corresponding perturbed and unperturbed sources.

Next consider a crystal identical to the above two-slip system material but with only the slip system at $\theta = 30°$. The evolution of $\|\delta\|$ with the number of dislocations is

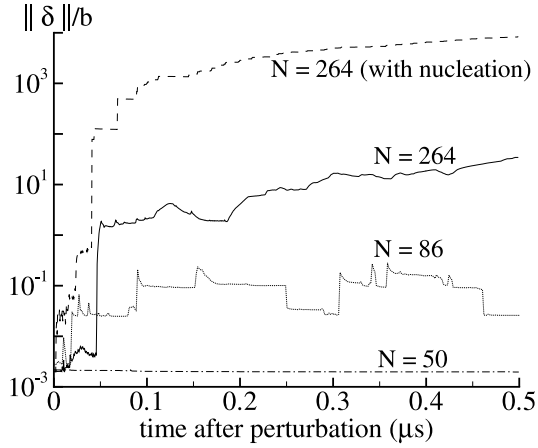

Fig. 3. Time evolution of $\|\delta\|$ with the nucleation of new dislocations switched-off for different values of the initial number of dislocations N. Also shown is a comparison calculation with $N = 264$ and the nucleation of new dislocations permitted.

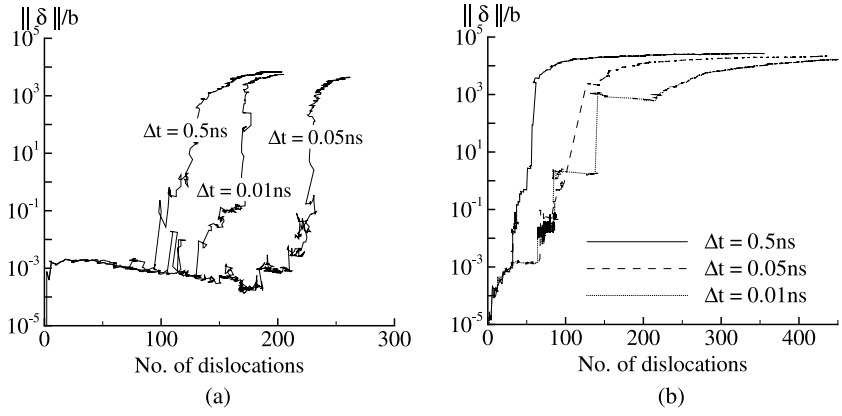

Fig. 4. Evolution of $\|\delta\|$ with number of dislocations (a) for a material with a single slip system at $\theta = 30°$, (b) the two-slip system material. Calculations employing three different time steps are shown in each case.

shown in Fig. 4a for computations carried out with time steps ranging from $\Delta t = 0.5$ to 0.01 ns. For these three cases, $\|\delta\|$ initially decreases (which implies a negative Lyapunov exponent) and then at some critical point abruptly rises. This critical point depends on the time step used and is thus indicative of a numerical instability. Note that the abrupt rise in $\|\delta\|$ seen in Fig. 4a occurs earlier with $\Delta t = 0.01$ ns than with $\Delta t = 0.05$ ns. This is because the numerical instabilities are a result of integration "overstepping" which give rise to oscillations at dislocation pile-ups. Hence the numerical instability is a local phenomenon rather than being associated with the total number of dislocations. Such integration instabilities which give rise to an increased Lyapunov exponent are also seen in molecular dynamic calculations [6]. Thus, at least over the range calculated, the single slip system material does not have a positive

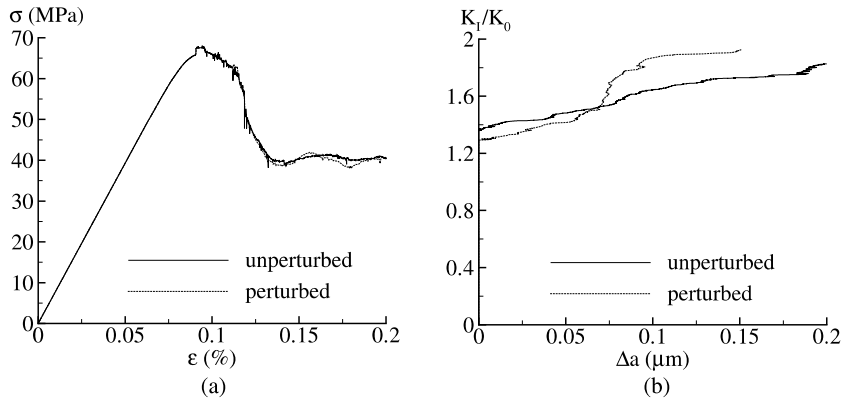

Fig. 5. (a) Stress versus strain response in uniaxial tension of the two-slip system material, (b) applied stress intensity factor K_I/K_0 versus crack extension Δa. Two calculations corresponding to (i) the unperturbed case and (ii) nucleation sites perturbed by $10^{-3}b$ are shown in each case.

Lyapunov exponent with the norm $\|\delta\|$ and the results in Fig. 4a give no evidence for chaos. While the same numerical instabilities as occur in single slip are possible in multislip, the growth of $\|\delta\|$ with the number of dislocations for the two-slip system case in Figs. 2a and 4b is relatively independent of the time step and the response converges as the time step is decreased. Based on dislocation dynamics simulations of creep in single slip with periodic boundary conditions, Miguel et al. [14] have obtained behavior consistent with a dissipative self-organized critical system.

The effect of chaotic dislocation behavior on the stress–strain response and the fracture toughness is illustrated in Fig. 5. The overall stress versus strain response of the two-slip system crystal subjected to uniaxial tension is shown in Fig. 5a for two cases (i) reference and (ii) nucleation sites perturbed by at most $10^{-3}b$. The difference in the overall macroscopic response in this case is negligible even though the dislocation positions in the two cases are quite different. This can be contrasted with the behavior of the fracture toughness which depends on local conditions. In Fig. 5b the crack growth resistance of a crystal is shown by plotting the applied normalized remote mode I stress intensity factor K_I/K_0 against the crack advance Δa (refer to Ref. [4] for details of these calculations). The crack growth resistance varies significantly with perturbations of $10^{-3}b$ in the positions of the nucleation sites.

Conclusions

Dislocation dynamics is chaotic and this chaotic nature depends on the density of dislocations, on the slip geometry and on the competition between nucleation and annihilation. Other factors that are likely to play a major role in determining the emergence of chaos include the specimen geometry and the loading conditions. In particular, under the tensile loading conditions analyzed, all the dislocations are statistical dislocations. In the crack problem, gradients lead to the presence of geometri-

cally necessary dislocations and there is the possibility that statistical and geometrically necessary dislocations play different roles in the development of chaos. The emergence of chaos is a consequence of dislocation motion, since the interaction of stationary dislocations is a problem in static elasticity, ruling out chaotic behavior. The role of the various dislocation interactions in promoting chaos remains to be determined. Also, the calculations here have used the linear drag relation (1) and the development of chaos can be quite sensitive to small changes in the prescription of the dynamics [7].

In Fig. 5a the chaotic nature of the motion of the discrete dislocations did not appreciably affect the overall stress–strain response, but it did affect the crack growth resistance in Fig. 5b. The conditions for crack growth are determined at small length scales and are much more sensitive to local variations. Identifying the sensitivity of material properties and behaviors to dislocation chaos is key for differentiating between controllable experimental scatter and the inherent variability of material response.

Acknowledgements

Support from the AFOSR MURI at Brown University on Virtual Testing and Design of Materials: A Multiscale Approach (AFOSR Grant F49620-99-1-0272) is gratefully acknowledged. VSD thanks the English Speaking Union for support through the Lindemann Fellowship.

References

[1] Kubin, L. P., Canova, G., Condat, M., Devincre, B., Pontikis, V., & Bréchet, Y. (1992). Solid State Phenom 23, 455.
[2] Van der Giessen, E., & Needleman, A. (1995). Model Simul Mater Sci Eng 3, 689.
[3] Zbib, H. M., Rhee, M., & Hirth, J. P. (1998). Int J Mech Sci 40, 113.
[4] Cleveringa, H. H. M., Van der Giessen, E., & Needleman, A. (2000). J Mech Phys Solids 48, 1133.
[5] Poincaré, H. (1899). Les méthodes nouvelles de la mécanique céleste. Paris: Gauthier-Villars.
[6] Edwards, R. G., Horváth, I., & Kennedy, A. D. (1997). Nucl Phys B 484, 375.
[7] Aref, H. (1983). Proceedings of the XIVth International Congress on Theoretical Applied Mechanics, Copenhagen, Ann Rev Fluid Mech 15, 345.
[8] Lorenz, E. N. (1963). J Atmos Sci 20, 130.
[9] Noronha, S. J., Ananthakrishna, G., Quaouire, L., Fressengeas, C., & Kubin, L. P. (1997). Int J Bifurcat Chaos 7, 2577.
[10] Kung, J. F., Bao, H., & Galligan, J. M. (1996). Scripta Mater 34, 479.
[11] Ananthakrishna, G., & Valsakumar, M. C. (1983). Phys Lett A 95, 69.
[12] Walgraef, D., & Aifantis, E. C. (1985). J Appl Phys 58, 688.
[13] Strogatz, S. H. (1994). Nonlinear Dynamics and Chaos, Reading, MA: Perseus Books.
[14] Miguel, M.-C., Vespignani, A., Zapperi, S., Weiss, J., & Grasso, J.-R. (2001). Nature 410, 667.